CrossMark

EMERGING TECHNOLOGIES

Vibrational microspectroscopy enables chemical characterization of single pollen grains as well as comparative analysis of plant species based on pollen ultrastructure

Boris Zimmermann[1] · Murat Bağcıoğlu[1] · Christophe Sandt[2] · Achim Kohler[1,3]

Abstract

Main conclusion **Chemical imaging of pollen by vibrational microspectroscopy enables characterization of pollen ultrastructure, in particular phenylpropanoid components in grain wall for comparative study of extant and extinct plant species.**

A detailed characterization of conifer (Pinales) pollen by vibrational microspectroscopy is presented. The main problems that arise during vibrational measurements were scatter and saturation issues in Fourier transform infrared (FTIR), and fluorescence and penetration depth issues in Raman. Single pollen grains larger than approx. 15 µm can be measured by FTIR microspectroscopy using conventional light sources, while smaller grains may be measured by employing synchrotron light sources. Pollen grains that were larger than 50 µm were too thick for FTIR imaging since the grain constituents absorbed almost all infrared light. Chemical images of pollen were obtained on sectioned samples, unveiling the distribution and concentration of proteins, carbohydrates, sporopollenins and lipids within pollen substructures. The comparative analysis of pollen species revealed that, compared with other Pinales pollens, *Cedrus atlantica* has a higher relative amount of lipid nutrients, as well as different chemical composition of grain wall sporopollenin. The pre-processing and data analysis, namely extended multiplicative signal correction and principal component analysis, offer simple estimate of imaging spectral data and indirect estimation of physical properties of pollen. The vibrational microspectroscopy study demonstrates that detailed chemical characterization of pollen can be obtained by measurement of an individual grain and pollen ultrastructure. Measurement of phenylpropanoid components in pollen grain wall could be used, not only for the reconstruction of past environments, but for assessment of diversity of plant species as well. Therefore, analysis of extant and extinct pollen species by vibrational spectroscopies is suggested as a valuable tool in biology, ecology and palaeosciences.

Keywords FTIR microspectroscopy · Raman microspectroscopy · Pinales · Imaging · Cell wall

✉ Boris Zimmermann
boris.zimmermann@nmbu.no

Murat Bağcıoğlu
murat.bagcioglu@nmbu.no

Christophe Sandt
christophe.sandt@synchrotron-soleil.fr

Achim Kohler
achim.kohler@nmbu.no

[1] Department of Mathematical Sciences and Technology, Faculty of Environmental Science and Technology, Norwegian University of Life Sciences, Drøbakveien 31, 1430 Ås, Norway

[2] Synchrotron SOLEIL, L'Orme des Merisiers, Saint-Aubin, BP 48, 91192 Gif-sur-Yvette, France

[3] Nofima AS, Osloveien 1, 1430 Ås, Norway

Introduction

Fourier transform infrared (FTIR) and Raman spectroscopy are powerful techniques for studying inorganic, organic and biological samples. During recent years, they have become very popular for the analysis of plants. The two techniques, commonly referred to as vibrational or molecular spectroscopy, offer chemical characterization of plant samples via identifiable spectral features. A vibrational spectrum of a plant sample contains specific

signatures of the constituent compounds, such as water, lipids, proteins, carbohydrates, pigments and complex biopolymers (Schulz and Baranska 2007). A major advantage of these techniques is that they can provide economical high-throughput analysis of biological samples without any chemical pre-treatment.

In vibrational microspectroscopy, infrared and Raman spectrometers are combined with a microscope to measure spectra of samples on a microscopic level. In microspectroscopy, spatially resolved measurements of a sample are obtained either by point-by-point measurements employing a single element detector ('mapping') or by the simultaneous measurement of the whole area by a focal plane array detector ('imaging'). The obtained image is often referred to as hyperspectral image since it contains information on hundreds of spectral channels (wavelengths). The image enables chemical interpretation of spatially resolved spectral signals. Thus, based on these specific signals, chemical images with spatial distribution of chemical components in the sample can be obtained. The spatial resolution of FTIR and Raman microspectroscopy is defined by the diffraction limit, which depends on the wavelength of the light of the source and the objective used. In Raman measurements, the lateral resolution is typically within the range of 0.3–1.0 μm, which is comparable to microscopes that are using light in the visible range. In FTIR spectroscopy, the diffraction limit is within the range of 2–20 μm due to the long wavelength of mid-infrared light (Lasch and Naumann 2006). However, such spatial resolution is rarely obtained with conventional IR sources and thus the typical lateral resolution is within the range of 20–50 μm. Regarding that plant cells are on average some of the largest eukaryotic cells, in general both techniques have sufficient spatial resolution for the analysis of plant cells and tissues. FTIR and Raman have been applied extensively on various plant structures, such as cell walls, seeds, and leaves, for research on plant physiology, developmental biology, genetics and ecology (Gorzsas et al. 2011; Barron et al. 2005; Dokken et al. 2005; Chen et al. 2013; Yu 2011; Gierlinger and Schwanninger 2006; Chylińska et al. 2014; Agarwal 2006; Fackler and Thygesen 2013; Gierlinger et al. 2012).

Plant pollen is microscopic and, therefore, its characterization and analysis has been almost exclusively performed within the domain of optical and electron microscopy. Pollen grains are multicellular male gametophytes of seed plants, that have vegetative and generative cells enclosed in a highly resistant cell wall. Pollen grains of various species can vary quite a lot in grain shape and size, number, type and position of apertures, and structure and sculpture of the grain wall. In the last decade, vibrational spectroscopy of pollen has been performed in macroscopic mode on bulk samples, resulting in the clear identification of main chemical constituents (Zimmermann and Kohler 2014; Zimmermann 2010; Parodi et al. 2013; Pappas et al. 2003; Gottardini et al. 2007; Schulte et al. 2008, 2009, 2010; Ivleva et al. 2005).

Unfortunately, although microspectroscopy of pollen appears as a natural extension of vibrational studies, the measurements are hampered by technical difficulties. Raman measurements of pollen are hindered by laser-induced degradation, as well as by the strong fluorescence background that often masks any underlying Raman spectra (Laucks et al. 2000; Boyain-Goitia et al. 2003; Ivleva et al. 2005). The problem of strong fluorescence in the Raman spectra of pollen can be circumvented by photobleaching, i.e., photodepletion of the carotenoid molecules (Ivleva et al. 2005; Schulte et al. 2008, 2009). However, the process not only destructs the sample partially, it also significantly increases the spectral acquisition time. An alternative solution is the application of FT-Raman spectroscopy employing a near infrared (NIR, 1064 nm) laser excitation (Zimmermann 2010). Unfortunately, the use of a near infrared laser excitation in FT-Raman spectroscopy results in a lower spatial resolution and sensitivity compared to dispersive Raman where lasers with wavelengths in the visible region are employed. In FTIR microspectroscopy of pollen we encounter strong scattering, since pollen are due to their size and shape highly scattering samples in the infrared. The strong light scattering results in anomalous spectral features that can significantly interfere with and distort the signals of chemical absorption (Lukacs et al. 2015; Dell'Anna et al. 2009). Since scatter issues are a direct result of pollen size and morphology, the same problems can be expected in FTIR measurements of other microorganisms that are enclosed in a hard shell, such as plant and fungal spores and diatom algae. Despite these difficulties, vibrational spectroscopy of pollen has been providing valuable new data, and can thus serve as a powerful biophysical technique particularly in environmental and plant development studies (Zimmermann and Kohler 2014; Schulte et al. 2010).

In the paper at hand, we present the study on chemical imaging and characterization of pollen grains by FTIR microspectroscopy brining pollen substructures and their chemical components, such as grain wall biopolymers, into focus. This is of importance since the concentration of phenylpropanoid components in wall biopolymers can be used as UV-B proxy and changes in the flux of UV-B radiation can be tracked over geological time (Lomax et al. 2012). Therefore, the aim of this study was to investigate to what extend FTIR and Raman microspectroscopy measurements can reveal spatially resolved chemical information of pure grain biopolymers of Pinaceae pollen. This would facilitate the analysis of these important compounds, which according to state-of-the-art technology are analyzed

following harsh chemical pre-treatment, which could alter their chemical composition (Wehling et al. 1989; Ahlers et al. 1999; Jungfermann et al. 1997). The study covers single grain FTIR measurements employing both globar and synchrotron light sources. The level of chemical information that can be obtained by spatially resolved FTIR spectroscopy is discussed and compared to Raman microspectroscopic measurements. Different methodologies for obtaining vibrational microspectroscopic data are discussed together with methods for multivariate analysis of the microspectroscopic data. The potential of vibrational imaging as a tool for studying pollen physiology is elucidated.

Results

FTIR measurements of intact pollen grains

Spectral anomalies hinder spectral reproducibility

In infrared microspectroscopy, pollen, cells and tissues are highly scattering samples since the sizes of samples are at the same order as the wavelength range employed in the infrared microspectroscopic measurements (Lukacs et al. 2015; Bassan et al. 2010a, b). For instance, Cupressaceae pollen grains have a uniform spheroidal morphology with diameters varying between 15 μm (*Juniperus*) to 35 μm (*Cunninghamia*), while the wavelength range of the mid-infrared light employed in the FTIR spectrometers is approx. 2.5–25.0 μm. Thus, spectra of single pollen grains, presented in Fig. 1, show substantial and complex anomalies. Compared with the spectra of bulk samples (multigrain samples), the single grain spectra of *Juniperus chinensis* have extensive anomalous signals. The strongest scattering anomalies were obtained in the microspectroscopy of single *Juniperus* grains while the weakest ones were obtained for *Cunninghamia* grains. This is as expected, since the sizes of *Juniperus* grains are exactly within the magnitude of the mid-IR light (Fig. 1). Since these anomalies origin from morphological and optical properties of the samples, infrared microspectroscopy of single grains having different morphological and/or optical properties, result in general in spectra with different scatter distortions. Since the same species can exhibit a variety of morphological characteristics, infrared spectra of single pollen grains from the same species, are not reproducible (Fig. 1c). The anomalous signals are distorting chemical absorbance signals, thus significantly hampering characterization of the sample. An additional problem is that the absorbance values of single pollen grains are often at the detection limit, as defined by signal-to-noise ratio. This means that conventional light sources (globar) cannot
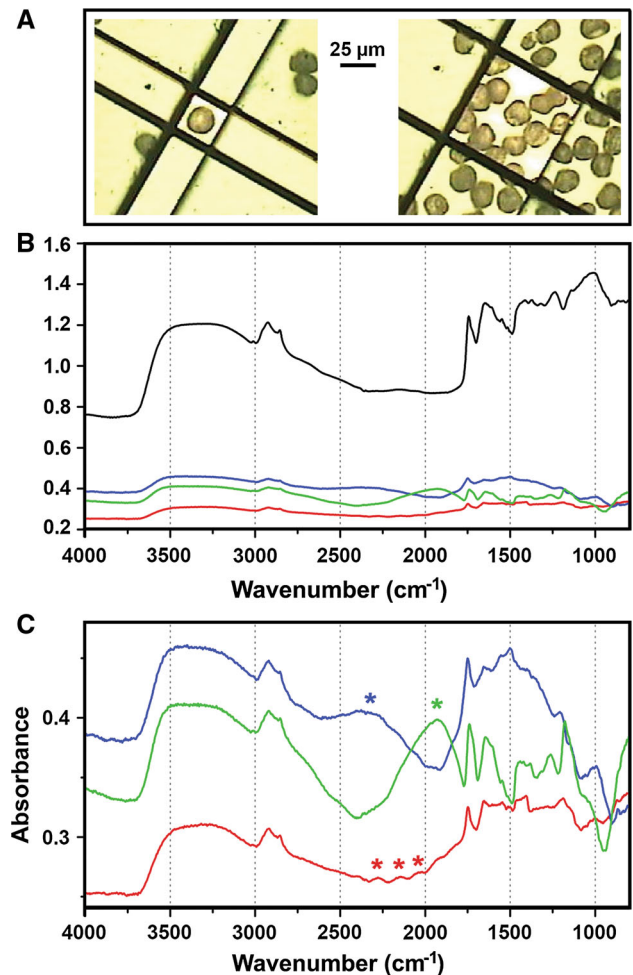

Fig. 1 Scattering anomalies in infrared spectra of pollen grains. **a** Optical microscope images of the measured *Juniperus chinensis* pollen grains on 3 mm ZnSe slide, with a 25 × 25 μm aperture for single grain measurement (*left*) and a 75 × 75 μm aperture for multigrain measurement (*right*). **b** Globar μFTIR spectra of *Juniperus chinensis*: multigrain spectrum (*black*), and single grain spectra of different grains (*blue*, *green* and *red*). **c** Enlarged single grain spectra from Fig. 1b; spectral artifacts due to scattering are designated with *asterisk*

provide quality spectra for small pollen grains, such is the case for measured species of *Juniperus* (Fig. 1).

Spatial oriented pollen samples hinder reproducibility

As opposed to Cupressaceae pollen grains, grains of Pinaceae have significantly larger diameters, ranging from 60 μm (*Podocarpus*) to 120 μm (*Abies*). In addition, their morphology is very complex: Pinaceae are described as saccate pollen due to a large hollow projection (saccus) from the central body of pollen grain (corpus). All measured Pinaceae species, as well as the Podocarpaceae species, have two sacci. The saccus regions, that can be easily depicted in the equatorial view (grain *a* in Fig. 2a),
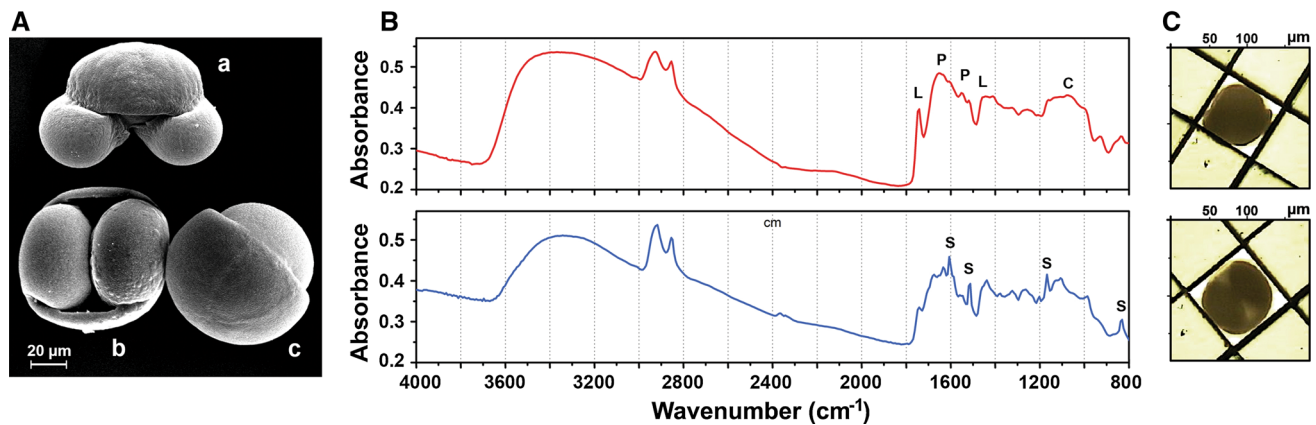
Fig. 2 Influence of spatial orientation of pollen samples on their infrared spectra. **a** SEM image of the intact *Abies cephalonica* pollen grains in: *a* equatorial front view, *b* distal polar view, and *c* equatorial profile view. **b** Globar μFTIR spectra of single pollen grains with equatorial profile orientation (*red*), and distal polar orientation (*blue*); the marked bands are associated with lipids (L), proteins (P), carbohydrates (C) and sporopollenins (S). **c** Corresponding optical microscope images of the measured pollen grains on 3 mm ZnSe slide, with depicted 100 × 100 μm aperture

are composed of sporopollenins only, a complex biopolymer. On the other hand, the corpus region contains nucleic acids and proteins, as well as nutrients in the form of lipids and sugars. As can be seen in Fig. 2b, measurements of Pinaceae single grains result in high-quality IR spectra that are devoid of scattering signals. However, we observe, that Pinaceae spectra are not reproducible due to differences in chemical absorption bands. The reason is that, Pinaceae samples do not have pseudo-radial symmetry as Cupressaceae grains, but rather distinct spatial orientations due to bilateral symmetry. The different orientations, corresponding to the infrared spectra in Fig. 2b, are shown in Fig. 2c (optical microscopy) and a (SEM measurement). It can be seen that the spectrum of the grain that has equatorial profile orientation has strong signals of lipids and proteins (Fig. 2b). Lipids are characterized by the strong vibrational band at 1745 cm^{-1} (C=O stretch), as well as by weaker bands at 1462 cm^{-1} (CH$_2$ deformation) (Gottardini et al. 2007; Pappas et al. 2004; Zimmermann 2010; Zimmermann and Kohler 2014). Proteins are characterized by two strong and broad bands at 1650 cm^{-1} (amide I: C=O stretch) and 1550 cm^{-1} (amide II: NH deformation and C–N stretch), while carbohydrates have strong absorption in 1200–900 cm^{-1} region (C–O–C and C–OH stretch) (Gottardini et al. 2007; Pappas et al. 2004; Schulte et al. 2008; Zimmermann 2010; Zimmermann and Kohler 2014). On the other hand, the spectrum of the grain that has distal polar orientation has strong signals of sporopollenins. The sporopollenin bands at 1605, 1515, 1171 and 833 cm^{-1} can be associated with the vibrations of aromatic rings (Zimmermann 2010; Schulte et al. 2008; Zimmermann and Kohler 2014). The reason for this discrepancy in spectral signatures of pollen for the two orientations is the spatial arrangement of the main biochemicals in Pinaceae pollen

grains. While the saccus regions are predominantly composed of sporopollenins, the corpus region is mainly composed of proteins, lipids and carbohydrates.

FTIR measurements of pollen substructures

For bigger pollen grains, even substructures on pollen grains can be measured by FTIR microspectroscopy. For instance, Pinaceae grains have sufficient sizes for more detailed measurements of grain substructures even by conventional IR light sources (globar). By choosing the desired aperture, IR microspectroscopy enables spatially resolved measurements of saccus and corpus substructures (Fig. 3a). The microspectroscopy data reveals the substantial biochemical differences between related Pinaceae genera *Cedrus* and *Abies*. The measurements show elevated relative lipid content in pollen interior belonging to *Cedrus* species, as compared to *Abies* (and other Pinaceae) species (Fig. 3b). More intriguing, though, is the extreme differences in biochemical composition of the grain wall (Fig. 3c). While *Abies* species show spectral features that are characteristic for the rest of the Pinaceae family (*Pinus* and *Picea* genera), *Cedrus* species display significant chemical deviation from this common wall composition. The difference indicates different chemical composition of sporopollenin biopolymers that build the exine layer of grain wall. The grain wall spectrum of *C. atlantica* shows bands at 852 and 815 cm^{-1}, which are both associated with ring vibrations of phenylpropanoid building blocks in sporopollenin (Schulte et al. 2008). The presence of these infrared bands indicates that *C. atlantica* has significant amount of ferulic building blocks in sporopollenins. In contrast, other measured Pinales pollens have sporopollenins composed almost exclusively of *p*-coumaric

Fig. 3 Measurement of infrared spectra of ultrastructure of pollen grain. **a** Optical microscope images of the measured *Abies cephalonica* pollen grain substructures, corpus (*left*) and saccus (*right*), on 3 mm ZnSe slide, with depicted 40 × 40 µm aperture. **b** Globar µFTIR spectra of corpus regions, and **c** saccus regions of *Cedrus atlantica*, *Abies cephalonica*, and *Picea abies*. For better viewing the spectra are offset. The marked bands are associated with lipids (L) and sporopollenins (S); the spectral regions of interest are denoted with *asterisks*
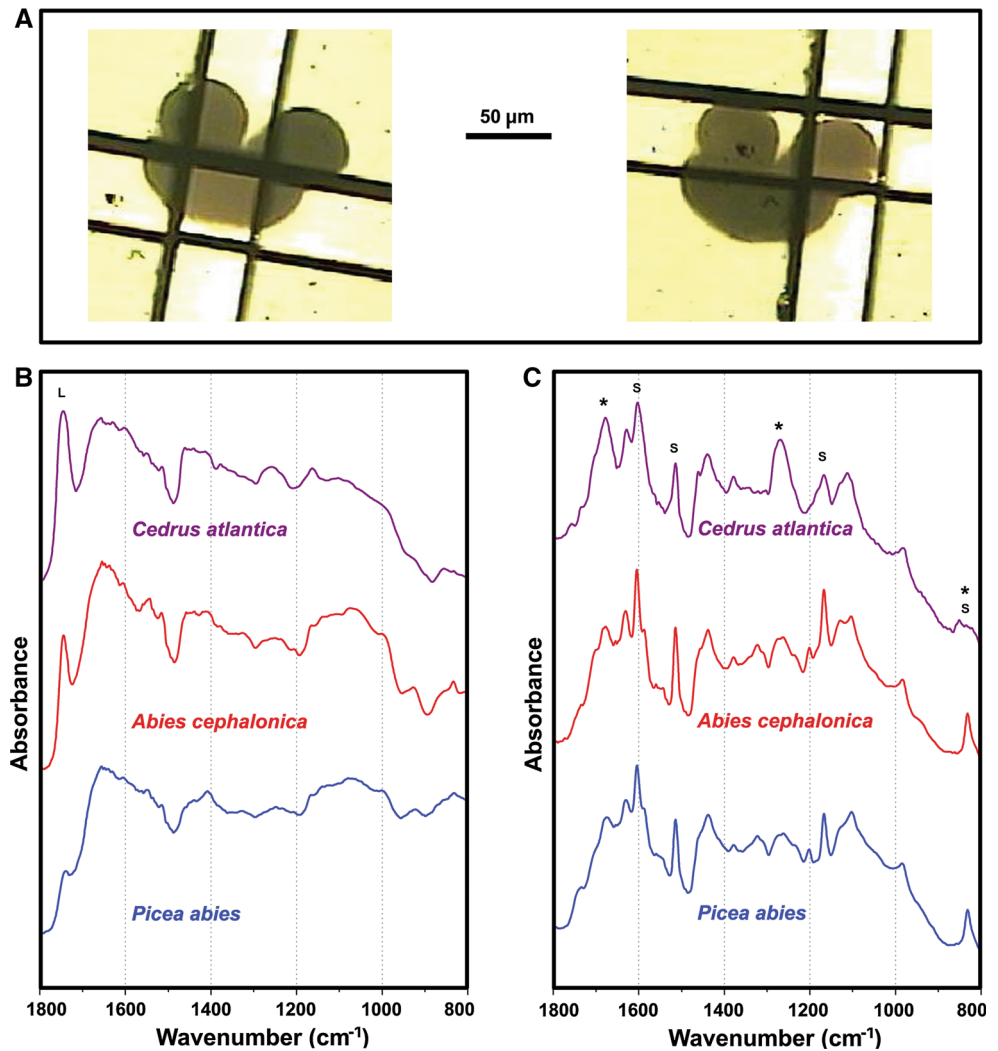
building blocks, as indicated by the strong band at 833 cm^{-1}. Phenylpropanoids play important role in mitigating damage caused by UV-B radiation, and thus their direct measurement from pollen grains, as described here, could be used to monitor effect of solar radiation on conifers (Blokker et al. 2006).

High-spatial resolution spectra of pollen substructures by synchrotron infrared spectroscopy

Synchrotron radiation light sources allow a more precise FTIR measurement of Pinaceae grains, such as line and image maps. As an example we show the line map of an intact *Abies cephalonica* pollen grain along the equatorial transect in Fig. 4. As can be seen, the chemical composition as well as the total absorption is changing substantially when moving from the hollow saccus region to the denser corpus region. Two phenomena can be observed when moving to the denser corpus region (red spectrum in Fig. 4b): (1) the scatter contributions increase considerable, and (2) the optical path length (thickness) of the sample becomes so high that the major part of the infrared light is completely absorbed. The spatially highly resolved synchrotron infrared spectra show that the central area of the corpus part of the grain is opaque for a large part of the infrared spectrum of the light. The small fraction of light that reaches the detector has passed through the periphery areas of corpus part, and thus cannot provide objective information about the grain interior. This allows us to draw an important conclusion for the spectra obtained from single Pinaceae pollen grains by conventional infrared microspectroscopy using globar sources as presented in Fig. 2: we expect that the globar measurements of the whole Pinaceae pollen grains presented above, are only in a little degree containing information about the corpus region. Spectral information is predominantly obtained from the saccus regions, since the saccus regions are transmitting more light than corpus region. This also
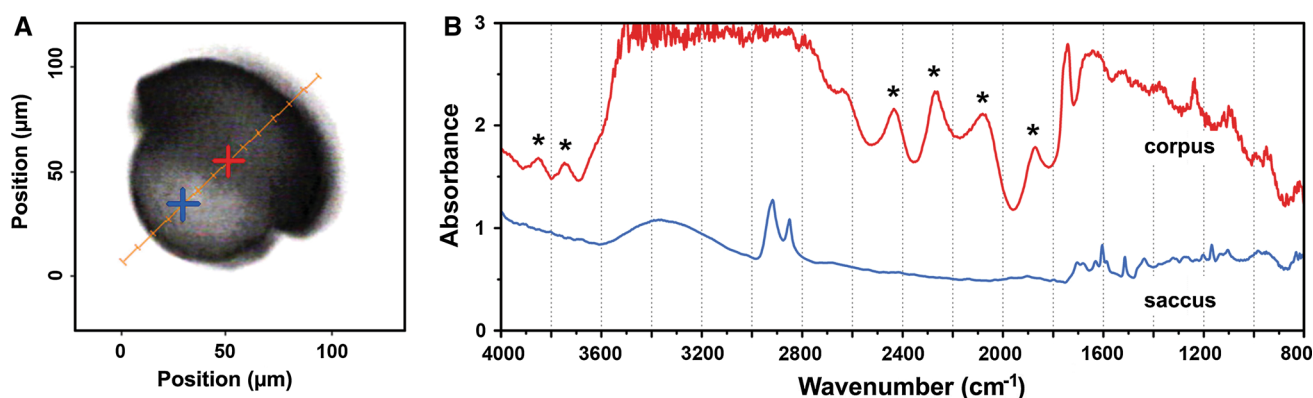
Fig. 4 Linear mapping of pollen grain by FTIR microspectroscopy. **a** Optical microscope image of the intact *Abies cephalonica* pollen grain in equatorial profile view, with positions of spectra acquisition: saccus (*blue*) and corpus regions (*red*). **b** Synchrotron µFTIR spectra, obtained with 20 × 20 µm aperture, of saccus (*blue*) and corpus regions (*red*) from Fig. 1a; spectral artifacts due to scattering are designated with *asterisk*

explains why the single grain spectra of Pinaceae pollen (see Fig. 2) are highly dependent on the grain spatial orientation during the measurement. The saturation effects revealed by synchrotron infrared spectroscopy with high brilliance employing small apertures, must be valid also for conventional infrared microscopy employing globar sources.

Vibrational measurements of sectioned pollen grains

As demonstrated above, large pollen grains, such as those of the family Pinaceae, are totally absorbing in the IR region. Thus, in order to obtain infrared spectra of such and similar-sized single pollen grains, the grains were sectioned to provide shorter optical path lengths. Following this strategy, FTIR images were obtained, where an image with a full FTIR spectrum in each pixel was obtained by mapping a whole image plane (Fig. 5) within 10 µm sections of Pinaceae grains embedded in optical cutting temperature compound (OCT) (Fig. 5). FTIR images, thus, represent large data sets, which can be displayed as pseudo color chemical images and associated with molecular composition of the sample. Chemical images are constructed by plotting intensity values of wavelength of interest (such as maxima of amide band), or alternatively by plotting ratio of band areas of signals of interest (such as ratio of amide band and sporopollenins ring vibration band in Fig. 5c, d). Construction of chemical image requires data processing, such as extended multiplicative signal correction (EMSC), for separation of chemical and physical spectral variations. For example, spectral variations can be caused by differences in the sample thickness, refractive index and other physical properties.

In addition to the infrared chemical images, Raman chemical images where obtained (Fig. 5). The quality of the Raman spectra obtained from thin sections was considerably better than previously obtained Raman spectra of intact grains (Zimmermann 2010): Since Raman spectroscopy is a scattering technique, spectra of intact grains show mainly signals from pollen grain wall components (Zimmermann 2010), while the Raman spectra of sections reveal molecular information about substructures of the cell interior. Another advantage of Raman spectroscopy of thin sections as opposed to whole grains was that grain sections suppressed strong fluorescence backgrounds in the Raman that may arise due to aromatic and polyenic compounds in grain wall.

It is worth noting that FTIR and Raman spectroscopy differ considerably in the spatial resolution they provide. For instance, in the µRaman measurement shown in Fig. 5, the acquisition laser light was focused on an area of 1 µm diameter, while the step size of motorized microscope stage in x and y directions was 2 µm. In the corresponding µFTIR measurement of the same sample, the synchrotron light was focused on an area of 10 × 10 µm due to resolution limitations. However, the small step size of microscope stage with 5 µm resulted in spatial oversampling and has improved the resolution. Regarding the nominal resolution, the µRaman measurement in Fig. 5c, has approximately seven times better nominal resolution than the µFTIR measurement in Fig. 5d, e (307 pixels per 1000 µm^2 in µRaman, versus 46 pixels per 1000 µm^2 in µFTIR).

As a general rule, the two methods obtain similar but complementary chemical information, since strong bands in the IR spectrum of a sample often correspond to weak bands in the Raman and vice versa. This is exactly what we observe in the vibrational spectroscopy of pollen, where strong Raman signals of sporopollenins are complemented by week signals in the infrared, while week Raman signals of lipids and proteins are countered by strong infrared signals of these compounds.
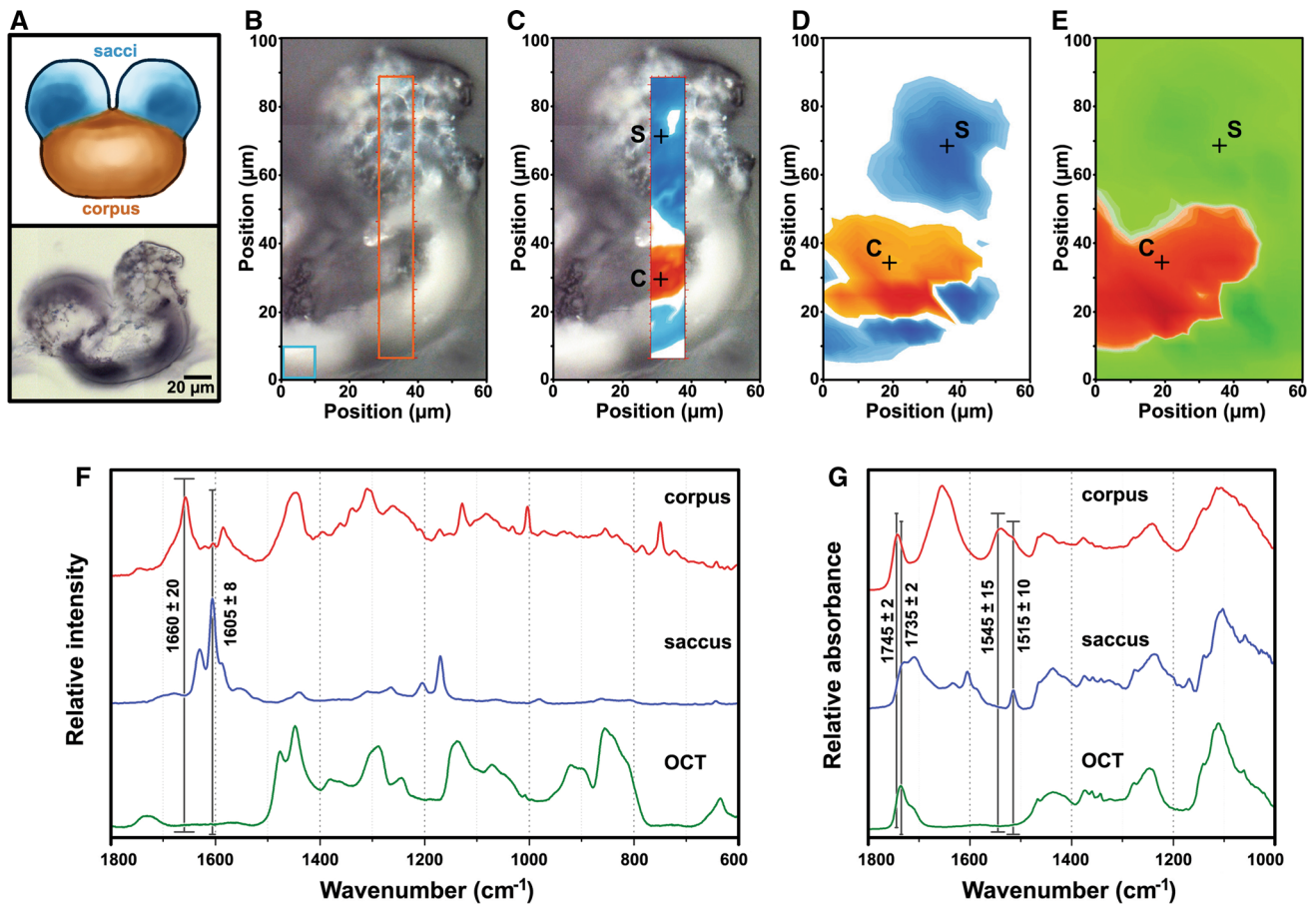
Fig. 5 Chemical images of pollen grain obtained by FTIR and Raman microspectroscopy. **a** Sketch in equatorial front view of a bisaccate Pinaceae pollen grain (*up*), and optical microscope image of the 10 μm section of *Abies cephalonica* pollen grain embedded in OCT on 1 mm ZnS slide (*down*). **b** Optical microscope image of the pollen grain showing the area (60×100 μm) for synchrotron μFTIR imaging (blue square represents 10×10 μm aperture; 5 μm FTIR step size); the area (10×82 μm) covered by μRaman imaging is depicted by orange rectangle (2 μm Raman step size). **c** μRaman image (overlaid on visible image) generated by the ratio of the areas under the amide I protein band (1660 ± 20 cm^{-1}) and the sporopollenin band (1605 ± 8 cm^{-1}); high ratio is depicted by *red* and low ratio by *blue colors* (see position of bands in Fig. 1f). **d** μFTIR image generated by the ratio of the areas under the amide II protein band (1545 ± 15 cm^{-1}) and the sporopollenin band (1515 ± 10 cm^{-1}); high ratio is depicted by *red* (high protein content) and low ratio by *blue colors* (high sporopollenin content); see position of bands in Fig. 5g. **e** μFTIR image generated by the ratio of the areas under the carbonyl lipid band (1745 ± 2 cm^{-1}) and the carbonyl OCT band (1735 ± 2 cm^{-1}); high ratio is depicted by *red* (high lipid content) and low ratio by *green colors* (high OCT content); see position of bands in Fig. 5g. **f** EMSC corrected Raman spectra of corpus and saccus pollen grain substructures (designated on Fig. 5c by C and S, respectively), and of OCT (see ratio of bands in Fig. 5c). **g** EMSC corrected IR spectra of corpus and saccus pollen grain substructures (designated on Fig. 5d, e by C and S, respectively), and of OCT (see ratios of bands in Fig. 5d, e). For better viewing the Raman and IR spectra are offset

The Raman chemical image in Fig. 5c shows clear spatial separation of sporopollenin constituents, characterized by the peak at 1605 cm^{-1} (aromatic ring stretches), and proteins, characterized by the peak at 1660 cm^{-1} (amide I band) (Schulte et al. 2008; Zimmermann 2010). Our results are corroborating findings obtained in the previous Raman chemical imaging, obtained on pollen of rye (*Secale cereal*) (Schulte et al. 2008). Due to larger radius and different symmetry, *Abies* pollen, compared to *Secale* pollen, shows clearer distinction between nutrient-rich regions (corpus) and sporopollenin-rich regions (grain wall, including saccus). However, the results are difficult to

compare since the two species belong to far related plant lineages with significant differences in chemical composition of pollen (Zimmermann and Kohler 2014).

A special attention has to be paid to the potential presence of signals belonging to the embedding OCT material in the measured Raman and FTIR spectra. Raman spectra of OCT exhibit week signals, and thus OCT signals are not interfering significantly with Raman signals of chemical constituents of pollen (Fig. 5f). In contrast, OCT has strong absorption bands in the infrared. Hence, OCT signals are present in the spectra of saccus and corpus regions. Although infrared signals of OCT interfere with the signals of

sporopollenins, lipids and proteins, there is still a sufficient number of specific peaks for the separation of information related to chemical pollen constituents. This is illustrated by the infrared chemical image presented in Fig. 5d. It was obtained by calculating the ratio of the protein band at 1545 cm^{-1} (amide II) and the sporopollenin band at 1515 cm^{-1} (aromatic ring vibration) (Zimmermann 2010; Zimmermann and Kohler 2014). The FTIR chemical image in Fig. 5d is complementary to Raman chemical image in Fig. 5c. In addition, an FTIR image was obtained by the ratio of the lipid band at 1745 cm^{-1} (carbonyl stretch) and the OCT band at 1735 cm^{-1} (carbonyl stretch) illustrating the spatial distribution of lipids (Fig. 5e).

Imaging and sample morphology

Vibrational imaging measurements are often affected by a number of unwanted phenomena, such as interfering effects of undesired physical variations. Regarding FTIR measurement of thin pollen sections (Fig. 5), there are two main sources of physical variations: changes in thickness within the section lead to variation in the effective optical path length, while chemical and physical inhomogeneity within the section lead to variations in the optical properties such as refraction and scattering. EMSC pre-processing enables estimation and separation of the undesired physical variations from the chemical information in the spectral data set (Kohler et al. 2005). For example, the chemical images in Fig. 5 were obtained after pre-processing with EMSC. In the EMSC model the unwanted physical information is explicitly parameterized (see Eq. 1), thus enabling detailed analysis of physical properties of a measured sample. Regarding that pollen grains have interesting physical properties, characterized by complex morphology of pollen ultrastructure, analysis of EMSC parameters offers an alternative approach for imaging of pollen grains.

Figure 6 illustrates the separation of physical and chemical information in FTIR images of pollen. The separation was obtained by using an EMSC model with constant, linear and quadratic parameters. The EMSC separates the recorded (original) spectrum (Fig. 6a) into a "corrected chemical spectrum" including chemical absorption bands (black spectrum in Fig. 6b), and physical information described by EMSC parameters (blue and red lines in Fig. 6b).

As can be seen from Fig. 6a, b the absorbance values of saccus and corpus regions differ substantially, with significantly weaker absorbance in the saccus region. The reason is aforementioned strong vibrational bands associated with lipids (carbonyl stretch) and proteins (amide I and amide II bands). On the other hand, sporopollenins are devoid of strong bonds, although they have characteristic bands at 1605 and 1515 cm^{-1}. The difference in total absorbance

between the two regions is mirrored by the difference in multiplicative parameters (b_i in Eq. 2) for the two regions: lower values of b for the saccus region and higher values for the corpus region. Moreover, the spectra belonging to different regions differ by other calculated EMSC parameters as well. For example, values for constant parameters (a_i in Eq. 2) have high positive values for the corpus region, low positive values for saccus region, and high negative values for the empty (OTC-only) region (Fig. 6d). In addition, values for the quadratic parameter (e_i in Eq. 2) have negative values for corpus region, and positive values for saccus region (Fig. 6e). These parameters correspond to baseline variations and may be explained by scattering phenomena. Thus, it is possible to construct scattering image of pollen's substructures by using only physical information, as described by EMSC parameters, and obtaining an image of morphological properties of substructures.

PCA imaging of pollen

Principal component analysis (PCA) is a multivariate data analysis method and is often the first method carried out on a multivariate spectral data set, such as vibrational spectra, for explorative data analysis. Since PCA allows interpretation based on all variables simultaneously, it enables more comprehensive visualization of spectral data. PCA transforms a spectral set from original variables (wavenumbers) into latent variables (principal components). The first component maximizes the co-variance in variable and sample space. Then, this first principal component is removed from the data set and the second component is found by maximizing the remaining co-variance and so on. The obtained principal components are uncorrelated. Typically, analysis of first few principal components is sufficient for obtaining a deeper understanding of the main variation patters that are present in spectral data since they capture the predominant part of the variance in the data. The relationship between original and latent variables is visualized by loading plots, which show how the different wavelengths contribute to the PCA model.

A PCA of a spectral image is shown in Fig. 7. As can be seen from Fig. 7b, c, PC scores can be associated with different chemical constituents of pollen grain. The loadings plot of the PC1 (Fig. 7d) has high negative values for signals associated with lipids (1745 cm^{-1}; carbonyl stretch) and proteins (1650 and 1550 cm^{-1}; amide I and amide II, respectively), and positive signals associated with the embedding OCT material (1500–1200 cm^{-1} region). In the PC1 image (Fig. 7b), the corpus region is characterized by high negative PC1 values, thus indicating that this region has a higher content of lipids and proteins. On the other hand, the loadings plot of the PC2 (Fig. 7d) shows high positive values for signals associated with sporopollenins (1605, 1515 and
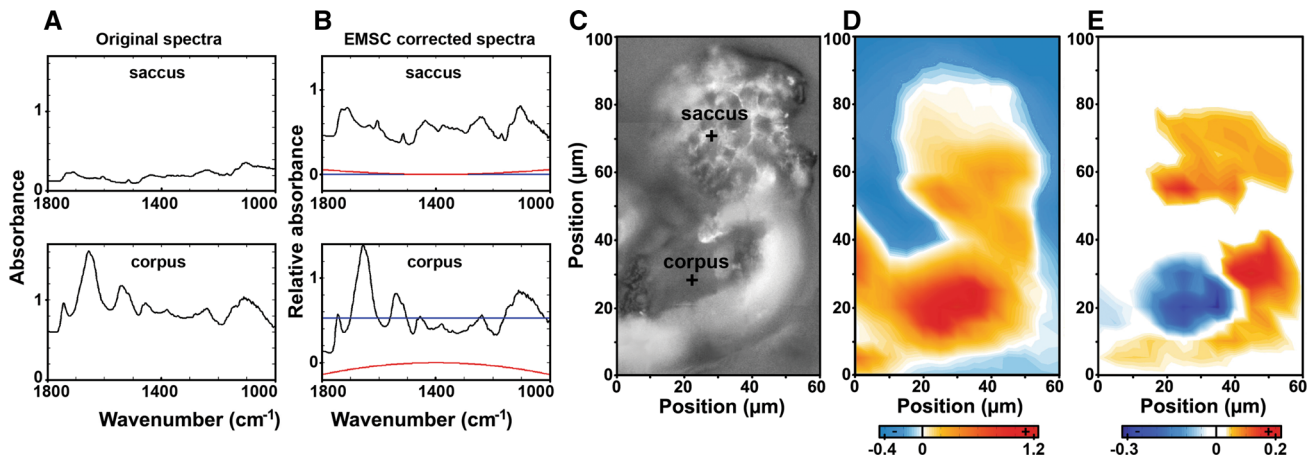
Fig. 6 Images obtained by separating chemical from physical information in the infrared spectra of *Abies cephalonica* pollen grain. **a** Original and **b** EMSC corrected IR spectra of corpus and saccus pollen grain substructures (designated on Fig. 5c); baseline (*a*) and quadratic (*e*) parameters are represented by *blue* and *red colors*, respectively. **c** Optical microscope image showing the area (60 × 100 μm) for μFTIR synchrotron imaging and the position of Fig. 2a, b spectra. Images of scattering properties: **d** constant baseline (*a*), and **e** quadratic baseline (*e*); negative and positive values are depicted by *blue* and *red colors*, respectively
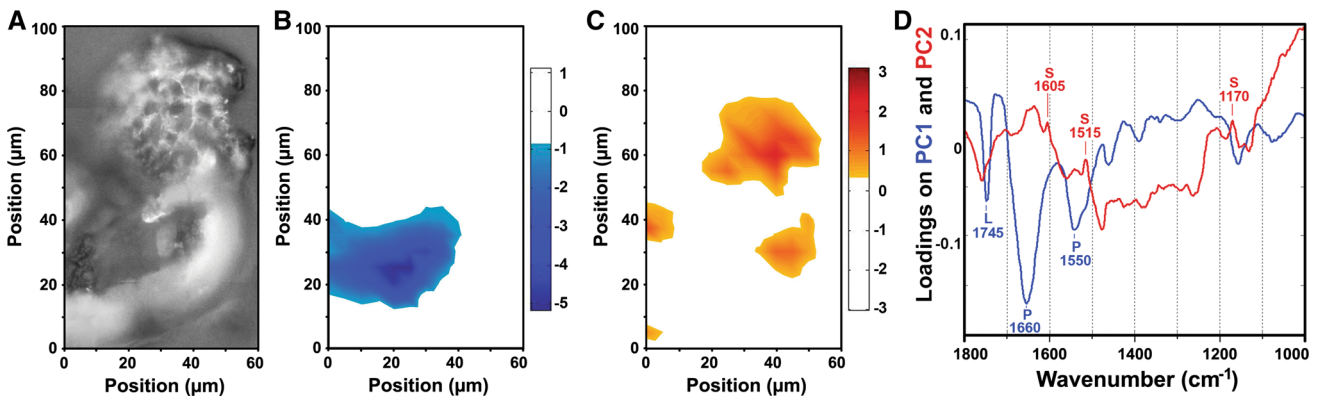

Fig. 7 Images obtained by principal component analysis of infrared spectral data. **a** Optical microscope image showing the area (60 × 100 μm) for μFTIR synchrotron imaging of the 10 μm section of *Abies cephalonica* pollen grain embedded in OCT on 1 mm ZnS slide. **b** Image of PC1 scores; high negative values are depicted by *blue color*. **c** Image of PC2 scores; high positive values are depicted by *red color*. **d** Loadings plot on the first two principal components of the PCA; the marked signals are associated with lipids (L), proteins (P) and sporopollenins (S). The percent variances for the first five PCs are 75.7, 9.8, 5.2, 2.5, and 1.9 %

1170 cm^{-1}; aromatic rings vibrations), and negative signals associated with OCT. In the PC2 image (Fig. 7c), the saccus region is characterized by high positive PC2 values; thus, indicating that this region has higher content of sporopollenins. Therefore, pseudo-chemical images of pollen grain sections can be obtained by using PCA information.

Discussion

Advantages and limitations of vibrational microspectroscopies of pollen

Different chemical constituents of pollen have different absorption coefficients, and thus different sub-regions of pollen have different propagation depths of infrared light. For example, proteins and lipids have higher absorption in the infrared region than grain wall components such as sporopollenins and cellulose. Therefore, grain regions with high concentration of grain wall components (such as saccus of Pinaceae grains) transmit more infrared light than grain regions rich in lipid nutrients (such as corpus of Pinaceae grains). This difference in infrared light absorption between different chemicals is mostly irrelevant for pollen grains with radial symmetry. However, for grains with bilateral symmetry, such as saccate pollen of Pinaceae family, it results in single grain spectra that are strongly dependent on grain spatial orientation (Fig. 2).

The biggest challenge in FTIR measurement of single pollen grains is the presence of anomalous signals due to

scattering (Figs. 1, 4). These signals are a major obstacle in the chemical interpretation of infrared spectra of single pollen grains. Spectral signatures of single pollen grains show strong Mie scattering due to their nearly perfect spherical shape (Lukacs et al. 2015). In comparison, nearly perfect absorbance spectra have been obtained, when plant materials have been probed by FTIR microspectroscopy as thin sections (Fackler and Thygesen 2013; Yu 2011). Mie scattering signatures are difficult to remove by spectral pre-processing methods. In an infrared spectrum, scattering and absorption signatures are highly entangled. The real and the imaginary part of the refractive index, that describe the optical and absorptive properties of the respective material, are connected through the Kramers–Kronig relation (Bassan et al. 2010a). This connection entangles the signatures of physical properties of the material and the chemical properties of the material in the measured absorbance spectrum. While the scatter signatures can give valuable information about size and density of pollen, the absorption signatures constitute a fingerprint of the biochemical components. Unfortunately, analytical solutions for complex structures, such as pollen grains, that would offer separation of scatter and absorbance components have not yet been developed (Lukacs et al. 2015). Therefore, spectra obtained from highly scattering samples contain strongly entangled chemical and physical information hampering the interpretation of the spectral signals.

Raman measurements of intact grains result in excessive representation of an external part of a grain due to a greater probability of multiplicative scattering in the grain interior (Zimmermann 2010). Therefore, Raman measurements of intact grains have disproportional bias toward pollen grain wall. For large pollen grains with thick grain walls, such as Pinaceae, it is unlikely that any constituent from the grain interior can be manifested in a spectrum. However, by sectioning a grain, pollen grain composition of the corpus region interior can be measured in detail (Fig. 5c).

Spectral pre-processing as a pre-requisite for chemical imaging

Light scattering is directly related to morphology, which can vary substantially in shape, size, and texture. Such morphology variation is typical for the measured Pinaceae samples: Saccus region of Pinaceae is characterized by sponge-like morphology of significantly lower density than one found within densely packed corpus region. Therefore, scattering features may serve as valuable information source for characterization of pollen, alongside chemical information. Figure 6 shows the separation of physical and chemical information in an FTIR image of pollen by using an EMSC model. The EMSC parameters are used to estimate non-chemical absorption, reflection and scattering of

light that is caused by irregularities within the pollen section. The pseudo-structural images, based on the representation of EMSC parameters (Fig. 6d, e), clearly show that their values are not random but rather specific for pollen ultrastructure. Therefore, alongside measurement of chemical composition of pollen ultrastructure, the FTIR methodology offers indirect estimation of physical properties. The indirect estimation of physical properties is not possible by filter-based pre-processing methods such as standard normal variate (SNV) (Barnes et al. 1989). EMSC, the model-based pre-processing method, allows the estimation of physical parameters, before removing them from spectra. While Multiplicative Signal Correction (MSC) only estimates a constant baseline (Ilari et al. 1988), EMSC in its basic form estimates in addition a linear and non-linear baseline. Compared to SNV and MSC, EMSC enables correction of wavelength-dependent scattering effects and thus provides better separation of physical and chemical information in vibrational spectra. The correlation of non-constant baseline variations with the physical properties of the sample is clearly demonstrated in Fig. 6e, where the quadratic baseline parameter reflects pollen ultrastructure by separating saccus and corpus regions.

Alongside EMSC-based imaging, PCA-based imaging of spectral data offers yet another rapid estimate of pollen chemical composition. As can be seen from Fig. 7, the most significant chemical information on pollen sections can be obtained by using PCA data analysis. The first two principal components are associated with lipids and proteins, as well as with sporopollenins (Fig. 7d). The PCA-based pseudo-chemical images of pollen grain sections show clear spatial distribution of these principal pollen constituents in either corpus or saccus substructures. The major value of such approach is significant reduction of data set by two orders of magnitude, from 400 frequency variables (wavenumbers) to only two latent variables (PCs 1 and 2) per spatial variable (measurement point).

Vibrational imaging as a tool for studying ultrastructure and physiology of pollen

The comparative analysis of Pinaceae genera shows substantial biochemical differences in the composition of grain wall, indicating different chemical composition of sporopollenins. The main difference in chemical composition of sporopollenins was obtained for *Cedrus*. In addition, *Cedrus* is unusual by quite high relative amount of lipid nutrients in grain corpus region. In this regard, *Cedrus* pollen have unique chemical composition with substantial deviation from *Abies*, its closest lineage. It should be noted however that *Abies* and *Cedrus* genera have diverged early in their evolutionary history, during Jurassic (∼183 Ma), approximately 30 Ma after the two branched from the rest

of Pinaceae lineage (Lin et al. 2010). Considering that *Abies* species have significantly larger grains (approx. 120 μm diameter for *Abies*, approx. 75 μm for *Cedrus*), this difference in nutrient concentration is possibly an adaptation of *Cedrus* to compensate the effect of relatively small grain size. *Cedrus* has one other unique feature connected to pollen: As opposed to other Pinaceae species that pollinate during spring, *Cedrus* shed pollen in autumn. It can be assumed that the large amount of lipid nutrients in grain interior, and the exceptional composition of grain wall, could play significant role in this unique pollination strategy. Measurement of sporopollenins can provide other valuable information as well. Grain wall sporopollenins are extremely resilient, thus preserving clear chemical fingerprint for at least several thousand years. It has been shown that this chemical fingerprint can be used for reconstruction of past climate, such as quantification of UV-B radiation flux through time using *Pinus* pollen from sediments (Willis et al. 2011). In this regard, vibrational microspectroscopy offers an alternative methodology for measurement of such chemical information, and thus has potential to significantly improve palaeoecological data.

Detailed chemical images of pollen can be obtained by cryosectioning and measurement either by Raman or synchrotron-based FTIR microspectroscopy. As demonstrated by chemical imaging of *Abies* in Fig. 5, spatial chemical information can be extracted by using characteristic bands of proteins, lipids, and sporopollenins. The FTIR chemical images were obtained even though OCT embedding matrix is not an optimal material for infrared spectroscopy (Fig. 5g). However, by carefully selecting ratios of characteristic bands it is possible to obtain clear chemical image of pollen OCT sections (Fig. 5d, e). On the other hand, OCT is suitable matrix material for Raman measurement of pollen due to weak Raman intensities of OCT bands (Fig. 5f). By measuring the same pollen section with the two vibrational microspectroscopies one can obtain complementary chemical images of pollen grain interior (Fig. 5). The acquired images, showing chemical heterogeneity of pollen interior with saccus and corpus regions, is a clear demonstration of the methods' potential for determining spatially resolved biochemical fingerprint of pollen ultrastructure.

In summary, in this paper, we presented an approach for chemical imaging of pollen grains by FTIR and Raman microspectroscopy. The main problems arising during measurements are scatter and saturation issues in FTIR, and fluorescence and penetration depth issues in Raman. Clear chemical images of pollen grain can be obtained by careful spectral pre-processing and analysis. Vibrational microspectroscopy studies can be used for measurement of an individual pollen grain, including measurement of grain ultrastructure. In theory, such studies would enable

measurement of within-plant and even within-flower biochemical variations of pollen grains in botany, as well as measurements of fossilized pollen samples from sediments. Therefore, chemical characterization of individual pollen grains by vibrational spectroscopies is suggested as a valuable tool in biology, ecology and palaeosciences.

Materials and methods

Plant material

Pollen samples were obtained through fieldwork at the Botanical Garden of the Faculty of Science, University of Zagreb. In total 24 samples were collected, belonging to 12 Pinales species during 2011 and 2012 pollination seasons. The sample set included six Pinaceae species: *Abies cephalonica* Loudon (Greek fir), *Cedrus atlantica* (Endl.) Manetti ex Carrière (Atlas cedar), *Picea omorika* (Pancic) Purk. (Serbian spruce), *Picea abies* (L.) H.Karst. (Norway spruce), *Pinus resinosa* Aiton (Red pine), *Pinus sylvestris* L. (Scots pine); five Cupressaceae species: *Cunninghamia lanceolata* (Lamb.) Hook. (China fir), *Cupressus sempervirens* L. (Mediterranean cypress), *Juniperus chinensis* L. (Chinese juniper), *Juniperus communis* L. (Common juniper), *Juniperus excelsa* M.Bieb. (Greek juniper); and one Podocarpaceae species: *Podocarpus neriifolius* D.Don (Brown pine). The pollen samples were collected directly from plants at flowering time by shaking male cones (strobili). The samples were kept in paper bags at r.t. for 24 h, and afterwards transferred to vials and stored at - 15 °C.

Sample preparation

Spectra of intact pollen grains were measured on ZnSe slides. Sectioned samples of pollen grains were obtained by embedding pollen in an optical cutting temperature compound (OCT, Tissue-Tek; Sakura Finetek, USA). The OCT samples were snap-frozen and sectioned at −20 °C using a cryostat (Leica CM 3050 S, Nussloch, Germany) obtaining sections of 10 μm thickness. The pollen sections were transferred to ZnS slides for measurements.

FTIR spectroscopy

FTIR microspectroscopy measurements were performed with globar and synchrotron sources. For each measured sample an image was recorded with an optical microscope.

Measurements with a globar source were performed on intact pollen grains in transmission mode with a spectral resolution of 4 cm^{-1}, using an Equinox 55 FTIR spectrometer with an IRScopeII IR microscope (Bruker

Optik GmbH, Germany). The system was equipped with a globar mid-IR source and a liquid nitrogen-cooled mercury cadmium telluride (MCT) detector. The spectra were measured in the 4000–600 cm^{-1} spectral range, with 128 scans for both background and sample spectra, using a 15× objective, with different aperture sizes, depending on the size of the sample. Background (reference) spectra were recorded immediately before starting each measurement using the sample-free setup. The Bruker system was controlled with OPUS 6.0 software (Bruker Optik GmbH, Germany).

Measurements with a synchrotron source were performed on intact and sectioned pollen grains at the SOLEIL synchrotron facility, on the SMIS infrared beamline, details of which can be found elsewhere (Dumas et al. 2006). The transmission spectra were recorded with a resolution of 4 cm^{-1} by using the synchrotron radiation coupled to a Nicolet 5700 FTIR spectrometer with a Nicolet Continuum XL IR microscope (Thermo Scientific, USA), equipped with a liquid nitrogen cooled mercury cadmium telluride detector. The spectra were measured in the 8000–650 cm^{-1} spectral range, with 128 scans for both background and sample spectra, using 15 × and 32 × objectives with different aperture sizes, depending on the size of the sample. The numerical aperture of the microscope was 0.65. Spectral maps were acquired as both linear maps and spectral images. For linear maps and images, steps sizes of 5 or 10 µm were used in a linear direction or in x and y directions, respectively. Background (reference) spectra were recorded immediately before starting each measurement using the sample-free setup. The Thermo system was controlled with OMNIC 8.1 software.

Raman spectroscopy

The Raman spectra were recorded using a DXR Raman Instrument (Thermo Fisher Scientific, Waltham, USA). Raman measurements were performed in a closed chamber using a stabilized 532 nm laser. The laser signal was generated by a Diode-pumped, solid state (DPSS) laser with 10 mW power, which was focused onto a 1.0 µm diameter spot, and measured in the spectral range of 125–3500 cm^{-1}. A 100 × objective (Thermo Fisher Scientific Waltham, USA) was used for focusing and collecting scattered Raman light. The confocal hole was set to 25 µm with a spectral resolution of 3.0 cm^{-1}. An exposure time of 2 × 10 s with 512 numbers of background exposures was used. A spectral map was acquired as spectral image, with a step size of 2 µm in x and y directions. Data acquisition and instrument control was carried out using the OMNIC 8.1 software (Thermo Fisher Scientific Inc, USA).

Data analysis

Data processing for chemical imaging was performed on the reduced wavenumber range, 1800–600 and 1800–1000 cm^{-1} for Raman and FTIR measurements, respectively. Each spectrum z_i (where $i = 1,..., N$; N is number of spectra in an image) was pre-processed by EMSC (Martens and Stark 1991). EMSC estimates and corrects baseline effects and multiplicative effects using the model.

$$z_i = b_i \boldsymbol{m} + a_i \boldsymbol{1} + d_i \widetilde{\boldsymbol{\nu}} + e_i \widetilde{\boldsymbol{\nu}}^2 + \boldsymbol{\varepsilon}_i \tag{1}$$

where $\boldsymbol{m}$ is the reference spectrum (typically an average spectrum or a representative spectrum), $\boldsymbol{1}$ is a vector containing ones as entries referring to a spectrum describing a constant baseline, $\widetilde{\boldsymbol{\nu}}$ a linear spectrum and $\widetilde{\boldsymbol{\nu}}^2$ a quadratic spectrum. The term $\boldsymbol{\varepsilon}_i$ describes the residual spectrum. The parameters a_i, b_i, d_i and e_i refer to constant, multiplicative, linear, and quadratic effects, respectively, and are estimated by least squares for each spectrum.

After having estimated the parameters, the spectra are corrected according to

$$\boldsymbol{z}_{i,Corr} = (z_i - a_i \boldsymbol{1} - d_i \widetilde{\boldsymbol{\nu}} - e_i \widetilde{\boldsymbol{\nu}}^2)/b_i \tag{2}$$

where $\boldsymbol{z}_{i,\text{Corr}}$ are the corrected spectra.

Pre-processed spectra were used to evaluate biochemical similarities between pollen samples by using principal component analysis (PCA). The spectral pre-processing and data analyses were performed by algorithms developed in house in the environment of Matlab, R2014a (The Mathworks Inc., Natick, United States) and The Unscrambler X 10.3 (CAMO Process AS, Oslo, Norway).

Scanning electron microscopy

The microscope images were recorded with a Zeiss EVO 50 Extended Pressure scanning electron microscope (Carl Zeiss AG, Jena, Germany). The desiccated pollen samples were attached to SEM stubs (covered with double-stick tape) without prior pre-treatment with chemicals. The samples were coated with gold–palladium and measured with SEM.

Author contribution statement BZ and AK conceived and designed the experiments. BZ, MB and CS performed the experiments. BZ, MB and AK analyzed the data. BZ, MB, CS and AK wrote the paper.

References

Agarwal UP (2006) Raman imaging to investigate ultrastructure and composition of plant cell walls: distribution of lignin and cellulose in black spruce wood (Picea mariana). Planta 224(5):1141–1153. doi:10.1007/s00425-006-0295-z

Ahlers F, Thom I, Lambert J, Kuckuk R, Wiermann R (1999) H-1 NMR analysis of sporopollenin from Typha angustifolia. Phytochemistry 50(6):1095–1098

Barnes RJ, Dhanoa MS, Lister SJ (1989) Standard normal variate transformation and de-trending of near-infrared diffuse reflectance spectra. Appl Spectrosc 43(5):772–777. doi:10.1366/0003702894202201

Barron C, Parker ML, Mills EN, Rouau X, Wilson RH (2005) FTIR imaging of wheat endosperm cell walls in situ reveals compositional and architectural heterogeneity related to grain hardness. Planta 220(5):667–677. doi:10.1007/s00425-004-1383-6

Bassan P, Kohler A, Martens H, Lee J, Byrne HJ, Dumas P, Gazi E, Brown M, Clarke N, Gardner P (2010a) Resonant Mie Scattering (RMieS) correction of infrared spectra from highly scattering biological samples. Analyst 135:268–277

Bassan P, Kohler A, Martens H, Lee J, Jackson E, Lockyer N, Dumas P, Brown M, Clarke N, Gardner P (2010b) RMieS-EMSC correction for infrared spectra of biological cells: extension using full Mie theory and GPU computing. J Biophotonics 3:609–620

Blokker P, Boelen P, Broekman R, Rozema J (2006) The occurrence of p-coumaric acid and ferulic acid in fossil plant materials and their use as UV-proxy. Plant Ecol 182(1–2):197–207. doi:10.1007/s11258-005-9026-y

Boyain-Goitia AR, Beddows DCS, Griffiths BC, Telle HH (2003) Single-pollen analysis by laser-induced breakdown spectroscopy and Raman microscopy. Appl Opt 42(30):6119. doi:10.1364/ao.42.006119

Chen J, Sun S, Zhou Q (2013) Direct observation of bulk and surface chemical morphologies of Ginkgo biloba leaves by Fourier transform mid- and near-infrared microspectroscopic imaging. Anal Bioanal Chem 405(29):9385–9400. doi:10.1007/s00216-013-7366-3

Chylińska M, Szymańska-Chargot M, Zdunek A (2014) Imaging of polysaccharides in the tomato cell wall with Raman microspectroscopy. Plant Methods 10(14):1–9

Dell'Anna R, Lazzeri P, Frisanco M, Monti F, Malvezzi Campeggi F, Gottardini E, Bersani M (2009) Pollen discrimination and classification by Fourier transform infrared (FT-IR) microspectroscopy and machine learning. Anal Bioanal Chem 394(5):1443–1452. doi:10.1007/s00216-009-2794-9

Dokken KM, Davis LC, Marinkovic NS (2005) Use of infrared microspectroscopy in plant growth and development. Appl Spectrosc Rev 40(4):301–326. doi:10.1080/05704920500230898

Dumas P, Polack F, Lagarde B, Chubar O, Giorgetta JL, Lefrançois S (2006) Synchrotron infrared microscopy at the French Synchrotron Facility SOLEIL. Infrared Phys Technol 49:152–160

Fackler K, Thygesen LG (2013) Microspectroscopy as applied to the study of wood molecular structure. Wood Sci Technol 47(1):203–222. doi:10.1007/s00226-012-0516-5

Gierlinger N, Schwanninger M (2006) Chemical imaging of poplar wood cell walls by confocal Raman microscopy. Plant Physiol 140(4):1246–1254. doi:10.1104/pp.105.066993

Gierlinger N, Keplinger T, Harrington M (2012) Imaging of plant cell walls by confocal Raman microscopy. Nat Protoc 7(9):1694–1708. doi:10.1038/nprot.2012.092

Gorzsas A, Stenlund H, Persson P, Trygg J, Sundberg B (2011) Cell-specific chemotyping and multivariate imaging by combined FT-IR microspectroscopy and orthogonal projections to latent structures (OPLS) analysis reveals the chemical landscape of secondary xylem. Plant J Cell Mol Biol 66(5):903–914. doi:10.1111/j.1365-313X.2011.04542.x

Gottardini E, Rossi S, Cristofolini F, Benedetti L (2007) Use of Fourier transform infrared (FT-IR) spectroscopy as a tool for pollen identification. Aerobiologia 23(3):211–219

Ilari JL, Martens H, Isaksson T (1988) Determination of particle-size in powders by scatter correction in diffuse near-infrared reflectance. Appl Spectrosc 42(5):722–728. doi:10.1366/0003702884429058

Ivleva NP, Niessner R, Panne U (2005) Characterization and discrimination of pollen by Raman microscopy. Anal Bioanal Chem 381(1):261–267. doi:10.1007/s00216-004-2942-1

Jungfermann C, Ahlers F, Grote M, Gubatz S, Steuernagel S, Thom I, Wetzels G, Wiermann R (1997) Solution of sporopollenin and reaggregation of a sporopollenin-like material: a new approach in the sporopollenin research. J Plant Physiol 151(5):513–519

Kohler A, Kirschner C, Oust A, Martens H (2005) Extended multiplicative signal correction as a tool for separation and characterization of physical and chemical information in Fourier transform infrared microscopy images of cryo-sections of beef loin. Appl Spectrosc 59(6):707–716. doi:10.1366/0003702054280649

Lasch P, Naumann D (2006) Spatial resolution in infrared microspectroscopic imaging of tissues. Biochim Biophys Acta 1758(7):814–829. doi:10.1016/j.bbamem.2006.06.008

Laucks ML, Roll G, Schweigers G, Davis EJ (2000) Physical and chemical (Raman) characterization of bioaerosols-pollen. J Aerosol Sci 31:307–319

Lin CP, Huang JP, Wu CS, Hsu CY, Chaw SM (2010) Comparative chloroplast genomics reveals the evolution of Pinaceae genera and subfamilies. Genome Biol Evol 2:504–517. doi:10.1093/gbe/evq036

Lomax BH, Fraser WT, Harrington G, Blackmore S, Sephton MA, Harris NBW (2012) A novel palaeoaltimetry proxy based on spore and pollen wall chemistry. Earth Planet Sci Lett 353:22–28. doi:10.1016/j.epsl.2012.07.039

Lukacs R, Blumel R, Zimmermann B, Bagcoglu M, Kohler A (2015) Recovery of absorbance spectra of micrometer-sized biological and inanimate particles. Analyst. doi:10.1039/C5AN00401B

Martens H, Stark E (1991) Extended multiplicative signal correction and spectral interference subtraction—new preprocessing methods for near-infrared spectroscopy. J Pharm Biomed 9(8):625–635. doi:10.1016/0731-7085(91)80188-F

Pappas CS, Tarantilis PA, Harizanis PC, Polissiou MG (2003) New method for pollen identification by FT-IR spectroscopy. Appl Spectrosc 57(1):23–27

Pappas D, Smith BW, Winefordner JD (2004) Raman imaging for two-dimensional chemical analysis. Appl Spectrosc Rev 35(1–2):1–23. doi:10.1081/asr-100101219

Parodi G, Dickerson P, Cloud J (2013) Pollen identification by Fourier transform infrared photoacoustic spectroscopy. Appl Spectrosc 67(3):342–348. doi:10.1366/12-06622

Schulte F, Lingott J, Panne U, Kneipp J (2008) Chemical characterization and classification of pollen. Anal Chem 80(24):9551–9556. doi:10.1021/Ac801791a

Schulte F, Mader J, Kroh LW, Panne U, Kneipp J (2009) Characterization of pollen carotenoids with in situ and high-performance thin-layer chromatography supported resonant Raman spectroscopy. Anal Chem 81(20):8426–8433

Schulte F, Panne U, Kneipp J (2010) Molecular changes during pollen germination can be monitored by Raman microspectroscopy. J Biophotonics 3(8–9):542–547. doi:10.1002/jbio.201000031

Schulz H, Baranska M (2007) Identification and quantification of valuable plant substances by IR and Raman spectroscopy. Vib Spectrosc 43(1):13–25. doi:10.1016/j.vibspec.2006.06.001

Wehling K, Niester C, Boon JJ, Willemse MTM, Wiermann R (1989) P-coumaric acid—a monomer in the sporopollenin skeleton. Planta 179(3):376–380

Willis KJ, Feurdean A, Birks HJ, Bjune AE, Breman E, Broekman R, Grytnes JA, New M, Singarayer JS, Rozema J (2011) Quantification of UV-B flux through time using UV-B-absorbing compounds contained in fossil Pinus sporopollenin. New Phytol 192(2):553–560. doi:10.1111/j.1469-8137.2011.03815.x

Yu P (2011) Microprobing the molecular spatial distribution and structural architecture of feed-type sorghum seed tissue (*Sorghum Bicolor* L.) using the synchrotron radiation infrared microspectroscopy technique. J Synchrotron Radiat 18(Pt 5):790–801. doi:10.1107/S0909049511023727

Zimmermann B (2010) Characterization of pollen by vibrational spectroscopy. Appl Spectrosc 64(12):1364–1373

Zimmermann B, Kohler A (2014) Infrared spectroscopy of pollen identifies plant species and genus as well as environmental conditions. PLoS One 9(4):e95417. doi:10.1371/journal.pone.0095417